# COB09-1252 - NUMERICAL SIMULATION OF FLOWS OVER A SMOOTH AND ROUGH HILL

**Ailson Santiago de Farias, ailsonfarias@gmail.com**
**José Luiz Alves da Fontoura Rodrigues, fontoura@unb.br**
University of Brasília CEP: 70.910-900 - Campus Darcy Ribeiro - Brasília - Distrito Federal - Brazil

***Abstract.****The main goal of this work is to simulate the flow developed on an abrupt rough hill. The numerical simulation were performed with a two-dimensional research code based on the finite elements method. The turbulence model adopted is the classical $\kappa$-$\varepsilon$ complemented by laws of wall, that consider the adverse pressure gradient and the wall roughness. The near wall treatment for rough surfaces was obtained adapting the laws of wall originally developed for smooth surfaces. The numerical profiles of mean velocity, mean pressure and friction velocity obtained with rough laws are compared with the numerical results given using the smooths laws and experimental data.*
***Keywords:*** *turbulence, rough surfaces, smooth surfaces, laws of wall, numerical simulation, finite elements*

## 1. INTRODUCTION

The turbulent flow established over rough surfaces has been experimentally studied since the beginning of 20th century. Nikuradse (1933) was one of the firsts to study this theme, derived relations for the shear stress in flows developed in rough surfaces. The rough element was placed artificially above the surfaces. So, the results obtained by Nikuradse (1933) for rough surfaces depends on the geometry of the sand-grain roughness. There's no information about the behavior of the flow over different kinds of rough surfaces. This way, the numerical and experimental results obtained by many researches for smooths surfaces are still applicable as a first approximation of the dynamic effects presenting in a turbulent flow over a rough surfaces.

Nowadays, the importance of this theme is increasing in industrial laboratories and academic centers. The literature shows many cases of direct numerical simulation (DNS) applied to rough surfaces with rectangular elements. The numerical simulation of the flow developed on rough surfaces is a very important research theme in order to improve the knowledge of atmospheric studies and industrial process. Ikeda and Durbin (2007) showed the direct numerical simulation of a channel with rough surface at one side, with rectangular ribs mounted, and smooth surface on the other side. The rough elements were mounted in order to attain sand-grain roughness. Ikeda and Durbin (2007) verified that, for high Reynolds numbers, the results obtained with logarithmic laws could be used in some cases by modifying the constants of the law and setting the correct origin for the velocity profile.

In this work, the numerical simulation of the turbulent flow over a rough surface was done by using the $\kappa$-$\varepsilon$ model, proposed by Jones and Launder (1972), with laws of wall, originally implemented to consider rough surface and now developed to consider also the near wall roughness, according to Loureiro et al (2007a) and Loureiro (2008). The numerical algorithmic adopted for the simulation, called Turbo2D, was written in Fortran and has been used and improved by Grupo de Mecânica dos Fluidos e Escoamentos Complexos - Vortex, from Mechanical Engeneering Department of the University of Brasília, since 1990. The isothermal variant was based in the finite elements method, using the treatment of Galerkin Method to convective fluxes. The spacial discretization was done by P1/ISOP2 elements. The temporal discretizantion used a semi-implicit sequential scheme of finite difference. The coupled equations, i.e., momentum and continuity equations, were solved using a variation of Uzawa's minimum residuals algorithm proposed by Buffat (1981).

## 2. GOVERNING EQUATIONS

### 2.1 $\kappa$-$\varepsilon$ turbulence model

The non-dimensional form of governing equations for a homogenous, one-phase and turbulent flow, composed by Reynolds equations and the classical $\kappa$-$\varepsilon$ model's equations are

$$\frac{\partial u_i}{\partial x_i} = 0 \tag{1}$$

$$\frac{\partial u_i}{\partial t} + u_j \frac{\partial u_i}{\partial x_j} = -\frac{\partial p}{\partial x_i} + \frac{1}{Fr} g_i + \frac{\partial}{\partial x_j}\left[\frac{1}{Re}\left(\frac{\partial u_i}{\partial x_j} + \frac{\partial u_j}{\partial x_i}\right) - \overline{u_i^{\prime} u_j^{\prime}}\right] \tag{2}$$

$$-\overline{u_i^{\prime} u_j^{\prime}} = \nu_T \left(\frac{\partial u_i}{\partial x_j} + \frac{\partial u_j}{\partial x_i}\right) - \frac{2}{3}\kappa \delta_{ij} \tag{3}$$

$$\nu_T = C_\mu \frac{\kappa^2}{\varepsilon} = \frac{1}{Re_T} \tag{4}$$

$$\left(\frac{\partial \kappa}{\partial t}+u_j\frac{\partial \kappa}{\partial x_j}\right)=\frac{\partial}{\partial x_j}\left[\left(\frac{1}{Re}+\frac{1}{Re_T\,\sigma_\kappa}\right)\frac{\partial \kappa}{\partial x_j}\right]+\varpi-\varepsilon \tag{5}$$

$$\left(\frac{\partial \varepsilon}{\partial t}+u_j\frac{\partial \varepsilon}{\partial x_j}\right)=\frac{\partial}{\partial x_j}\left[\left(\frac{1}{Re}+\frac{1}{Re_T\sigma_\varepsilon}\right)\frac{\partial \varepsilon}{\partial x_i}\right]+\frac{\varepsilon}{\kappa}\left(C_{\varepsilon1}\varpi-C_{\varepsilon2}\varepsilon\right) \tag{6}$$

$$\varpi=\left[\left(\frac{1}{Re_T}\right)\left(\frac{\partial u_i}{\partial x_j}+\frac{\partial u_j}{\partial x_i}\right)-\frac{2}{3}\kappa\delta_{ij}\right]\frac{\partial u_i}{\partial x_j} \tag{7}$$

where the non-dimensional variables $u$, $p$, $x_i$,$g_i$, $t$, $\nu_T$, $Re$,$Re_T$,$Fr$, $\kappa$, $\varepsilon$ and $\delta_{ij}$ represent, respectively, the mean velocity, a general pressure,the cartesian coordinate, the gravitational acceleration, the time variable, the eddy viscosity, the Reynolds number, the turbulent Reynolds number, the Froude number, the turbulent kinetic energy, the dissipation rate of turbulent kinetic energy and the delta of Kronecker.

The Reynolds' stress $-\overline{u_i^{'}u_j^{'}}$, defined by the law of Prandtl-Kolmogorov, represents the mean value of momentum's rate transfer caused by turbulent velocity's fluctuations.

Besides using the classical $\kappa$-$\varepsilon$ model, proposed by Jones and Launder (1972) with modifications introduced by Launder and Spalding (1974), it was implemented a modified form of the $\kappa$-$\varepsilon$ model proposed by Iaccarrino and Poroseva (2001). The focus of this form is the turbulent kinetic transport equation, changing the model coefficients in order to get more appropriated constants' values for each application, such as separated flows, strong adverse pressure gradient or specials geometric parameters. The group of constants, calibrated for periodic wavy channel flow, was chosen according to similarity criteria. The Table 1 shows the two groups of $\kappa$-$\varepsilon$ model constants.

Table 1. $\kappa$-$\varepsilon$ model constants

| Constant | Classical form | Modified form |
|---|---|---|
| $C_\mu$ | 0,09 | 0,09 |
| $C_{\varepsilon1}$ | 1,44 | 1,5 |
| $C_{\varepsilon2}$ | 1,92 | 1,92 |
| $\sigma_\kappa$ | 1,00 | 1,00 |
| $\sigma_\varepsilon$ | 1,3 | 0,67 |

## 2.2 Laws of the wall

The inner part of the turbulent boundary layer can be divided in three parts: viscous layer, buffer layer and turbulent layer, also called log region. Due to the $\kappa$-$\varepsilon$ model's incapacity to simulate the nearest wall part of the boundary layer, i.e., viscous layer, buffer layer and the initial part of turbulent region, this region is modelled by the relations called laws of the wall. Its function is only to calculate the boundary conditions of velocity, in the mesh's boundary that represents the walls. There are two kinds of laws of wall implemented in this study: the smooth and rough laws. The results of smoothes laws are showed in order to test the capability of these to simulate the flow over a rough surface and also to compare the effect of rough wall formulations in the near wall region.

The smoothes laws of the wall used were: the logarithmic law, the law of Mellor (1966), the law of Nakayama and Koyama (1984) and the law of Cruz and Silva Freire (1998). The rough laws, implemented and tested in this study, were: the law of Sholz (1925), the adapted forms of the law of Mellor (1966), the law of Nakayama and Koyama (1984) and the law of Cruz and Silva Freire (1998) for separating flows over a rough surfaces, developed by Loureiro el al (2007a) and Loureiro (2008).

The logarithmic law is based on the momentum transport equation of Prandtl for two dimension turbulent boundary layers, given by

$$\frac{\partial}{\partial y}\left(\nu\frac{\partial u}{\partial y}-\overline{u'v'}\right)-\frac{1}{\rho}\frac{\partial p^+}{\partial x}=0 \tag{8}$$

where $x$ and $y$ represents the normal and tangential directions, $p^+$ is the thermodynamic pressure and $\rho$ is the fluid density.

Disregarding the pressure gradient in the longitudinal direction and the viscous term on Equation (8), a double integration gives the classical logarithmic law for the turbulent region. Applying the Boussinesq assumption and the Prandtl's mixing length hypothesis, this law of the wall may be written in the form

$$u^*=\frac{1}{\varsigma}lny^*+C \tag{9}$$

where $\varsigma$ is the Von Kármán constant equal to 0.419 and C is an experimental calibration constant, equal to 5,445. The terms $u^*$ and $y^*$ are non-dimensional parameters, defined as

$$u^* = \frac{u}{u_F} \tag{10}$$

$$y^* = \frac{y u_F}{\nu} \tag{11}$$

where the term $u_F$ is a velocity scale, called friction velocity, originated during the deduction of the logarithmic law as constant of integration.

The law of Mellor (1966), on its original deduction for smooth surfaces, considers the adverse pressure gradients. The Eq.(8) is integrated on normal wall direction including the pressure term and disregarding the viscous stress term. The relation for the turbulent region is

$$u^* = \frac{2}{\varsigma}\left(\sqrt{1+p^*y^*}-1\right) + \frac{1}{\varsigma}\left(\frac{4y^*}{2+p^*y^*+2\sqrt{1+p^*y^*}}\right) + C_I \tag{12}$$

where

$$p^* = \frac{1}{\rho}\frac{\partial p}{\partial x}\frac{v}{u_F^3} \tag{13}$$

The Table (2) gives the constant of integration $C_I$ values as a function of $p^*$.

Table 2. Relation between $C_I$ e $p^*$

| $p^*$ | -0,01 | 0,00 | 0,02 | 0,05 | 0,10 | 0,20 | 0,25 | 0,33 | 0,50 | 1,00 | 2,00 | 10,00 |
|---|---|---|---|---|---|---|---|---|---|---|---|---|
| $C_I$ | 4,92 | 4,90 | 4,94 | 5,06 | 5,26 | 5,63 | 5,78 | 6,03 | 6,44 | 7,34 | 8,49 | 12,13 |

If ($p^* \geq 8$), the $C_I$ is given by the equation

$$C_I = \frac{2}{\varsigma} + 1,33(p^*)^{\frac{1}{3}} + 4,38(p^*)^{\frac{1}{3}} - \frac{1}{\varsigma}\ln\left(\frac{4}{p^*}\right) \tag{14}$$

The law of Nakayama and Koayama (1984) deduction begins at mean turbulent kinetic energy equation. Many steps after and according to Stratford (1959) study, the non-dimensional velocity at the near wall region is

$$u^* = \frac{1}{\vartheta}\left[3\left(\xi-\xi_s\right) + ln\left(\frac{\xi_s+1}{\xi_s-1}\frac{\xi_s-1}{\xi_s+1}\right)\right] \tag{15}$$

where

$$\xi = \sqrt{\frac{1+2\tau^*}{3}} \quad \text{e} \quad \tau^* = \frac{\tau}{\tau_w} = 1 + p^*y^* \tag{16}$$

$$y_s^* = \frac{e^{\varsigma C}}{1+p^{*n}} \tag{17}$$

with $n$ is equal to 0,34.

The law of Cruz and Silva Freire (1998) considers the asymptotic behavior of the boundary layer, near and far the recirculation zone, given by

$$u = \frac{\tau_p}{|\tau_p|}\frac{2}{\varsigma}\sqrt{\frac{\tau_p}{\rho}+\frac{1}{\rho}\frac{dP_p}{dx}y} + \frac{\tau_p}{|\tau_p|}\frac{u_F}{\varsigma}\ln\frac{y}{L_c} \tag{18}$$

where the sub-index $p$ indicates the properties at the wall, $u_R$ is the reference velocity and the term $L_c$ is

$$L_c = \frac{\sqrt{(\frac{\tau_p}{\rho})^2 + 2\frac{\nu}{\rho}\frac{dP_p}{dx}u_R} - \frac{\tau_p}{\rho}}{\frac{1}{\rho}\frac{dP_p}{dx}} \tag{19}$$

The Equation (18) has a logarithmic form for low pressure gradient, far from the recirculation zone. On the other hand, close to the high pressure gradient, near the separation and reattachment points, it tends to law of Stratford (1959).

The adjustment for the rough case is done by replacing the non-dimensional parameters, relating to velocity, pressure gradient and the cartesian y coordinate.

The rough law of Sholz (1925) is a logarithmic law that consider the roughness effect. For engineering applications, the Sholz's equation for rough surfaces is given by

$$u^* = \frac{1}{\varsigma} \ln(\frac{y}{y_s}) + C_r \tag{20}$$

where $C_r$ is equal to 8.5 and $y_s$ is the sand roughness, defined by Nikuradse (1933) as a function of geometric parameters of the roughness.

Besides sand roughness $y_s$, another important parameter used to model the roughness' effect is the error in origin $h_0$ for the velocity profile, calculated according to Perry and Joubert (1963). This parameter executes an important task indicating the best origin to the velocity profile, even in the explicit or implicit form in the laws of the wall. The technique used to determinate $h_0$ is done by displacing the origin until the experimental velocity profile presents a logarithmic fit, like the turbulent region of boundary layer's inner part. The physical reason for this adjust is the extinction of viscous sublayer. The Figure (3) shows the error in origin $h_0$ applied to the near rough wall boundary layer.

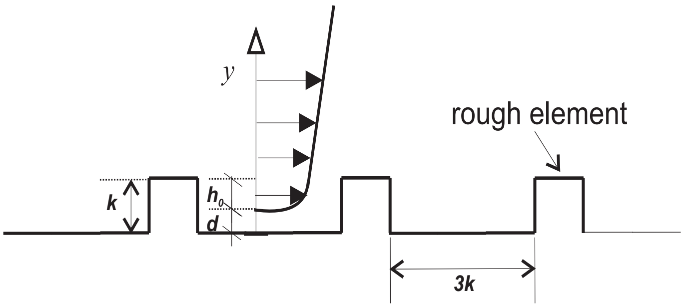


Figure 1. Roughness and the velocity profile origin.

This way, $y_s$ refers to the roughness' geometry and the error in origin $h_0$ refers to the dynamic's flow parameters in the near wall region.

The adjustment of the law of Mellor (1966) for the rough form is done replacing the non-dimensional parameters of length, velocity and pressure. For low longitudinal pressure gradient

$$y^* = \frac{y}{y_s} \tag{21}$$

$$p^* = \frac{y_s}{\rho} \frac{1}{u_F^2} \frac{\partial p}{\partial x} \tag{22}$$

The velocity scale depends on the longitudinal pressure gradient. For $p^* < 8.0$, the non-dimensional velocity is given by

$$u = \frac{u}{u_F} \tag{23}$$

The velocity scale for $p^* \geq 8.0$, $u_{rl}$, is estimated according to Stratford's equation (1959), giving the following relation

$$u = \frac{u}{u_{rl}} \tag{24}$$

with

$$u_{rl} = \sqrt{\frac{y_s}{\rho} \frac{\partial p}{\partial x}} \tag{25}$$

The rough form of the law of Nakayama e Koyama (1984) is direct obtained just using the non-dimensional parameters $y^*$ and $p^*$ for rough surfaces. The constant $C$, Eq.(17), should be replace with $C_r$, Eq.(20).

The law of Cruz and Silva Freire (1998) for rough surfaces is

$$u = \frac{\tau_p}{|\tau_p|} \frac{2}{\varsigma} \sqrt{B \frac{\tau_p}{\rho} + \frac{1}{\rho} \frac{dP_p}{dx} y} + \frac{\tau_p}{|\tau_p|} \frac{u_F}{\varsigma} \ln \frac{y}{L_c} \tag{26}$$

where the sub-index $p$ indicates the properties at the wall, $u_R$ is the a reference velocity, the constant $B$ is equal to 2.89 and the term $L_c$ is

$$L_c = \frac{\sqrt{(\frac{\tau_p}{\rho})^2 + 2\frac{y_s}{\rho}\frac{dP_p}{dx}u_R^2} - \frac{\tau_p}{\rho}}{\frac{1}{\rho}\frac{dP_p}{dx}} \tag{27}$$

As the longitudinal pressure gradient decreases, the Eq.(26) must tends to law of Sholz (1925). This asymptotic behavior was implemented chosen the correct value for the constant $B$.

## 3. NUMERICAL TREATMENT

The spacial discretization is done by triangular finite elements with linear interpolation functions, using the Galerkin Method. Two meshes were implemented: a basic mesh to calculate de pressure field, with P1 elements; and a fine mesh used to calculated the other variables, with P1/isoP2 elements and obtained by division from each P1 element into four equal elements. The basic mesh P1 is used to calculate the pressure field and, for this reason, is called pressure mesh. It has 1456 nodes and 2678 elements. In its turn, the fine mesh P1/isoP2 is used to calculate the velocity and all other variables, called velocity mesh. It has 5589 nodes and 10712 elements. The mesh generation was made using information about the solution structure. Thus, in the near wall region was used a dense grinding. On the other hand, in the outer part of the boundary layer, the nodes were more separated from each other, especially in the vertical direction. In order to minimize the discretization error, it was done an iterative refinement in the basic mesh, until the negligible variations in numerical results is reached.

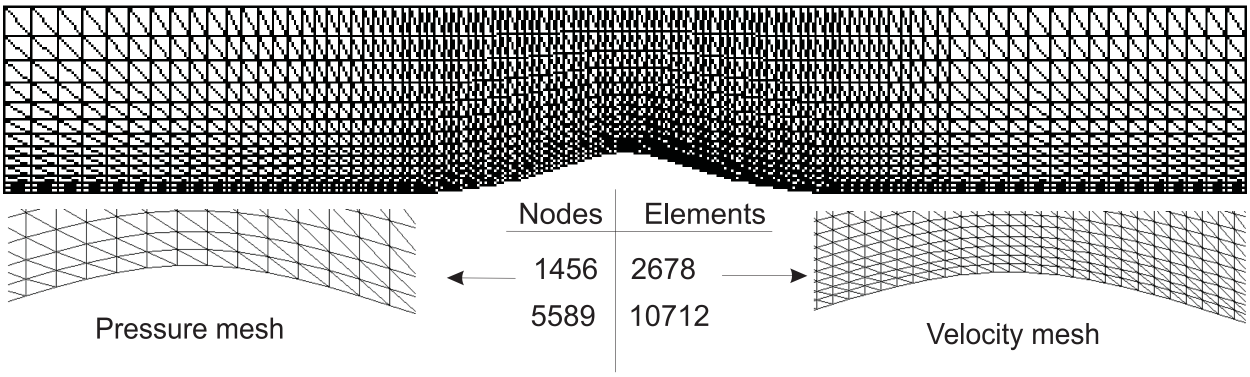


Figure 2. P1 and P1/ISO P2 meshes.

The temporal discretization of the equations' system is done by using a first order approximation for the temporal derivative. The algorithmic adopted allows the governing equations' linearization for each time step time.

The test case selected was the flow over an abrupt rough hill, studied by Monteiro (2007) and Loureiro (2008). The experimental result was obtained in a water channel with 17m length and transversal section of 0.4m by 0.6m. The rough effect was simulated putting rectangular bars in the bottom of the channel. The rectangular bars were made with rubber and placed in traversal form. These elements had transversal sectional square and equal to 9 $mm^2$ . They were separated by each other from 9mm. This case shows the turbulent phenomena that occur in a open-channel water flow, like recirculation zone and low pressure gradient regions. This fact permits a deep analysis of the physical congruity's numerical formulation adopted for the rough case, in a equilibrium boundary layer sense. This same test case with smooth wall was numerically and experimentally studied by Loureiro et al (2007) and Soares and Fontoura Rodrigues (2005). The numerical results showed in their works were solved by using Turbo2D, with smooth laws of wall. A great numerical results were obtained in the near wall region, especially the mean velocity field and the recirculation zone prediction, even working with the limitations of the $\kappa$-$\varepsilon$ model. This performance became possible due to use laws of wall that consider the adverse pressure gradient. The Table (3) and Figure (3) show the boundary conditions, the simulation parameters, the numerical domain and the measure station's location.

## 4. RESULTS

The numerical results were compared with the experimental data, for the mean velocity field, wall friction velocity, recirculation zone and pressure field. These results were used to validate the rough laws of the wall formulations.

The numerical results at station 2, upstream from the hill, obtained with rough laws showed in Fig.(5), is better than

Table 3. Flow parameters.

| | |
|---|---|
| Reference velocity, $U_0$ (m/s) | 0.3133 |
| Height of the hill, h (mm) | 60 |
| Boundary layer thickness, $\delta$ (mm) | 100 |
| Reynolds number, $Re_\delta$ | 31023 |
| Friction velocity, $u_F$ (m/s) | 0,02254 |
| Sand roughness, $y_s$ (mm) | 0.0138966 |
| Error in origin, $h_0$ (mm) | 1.1 |

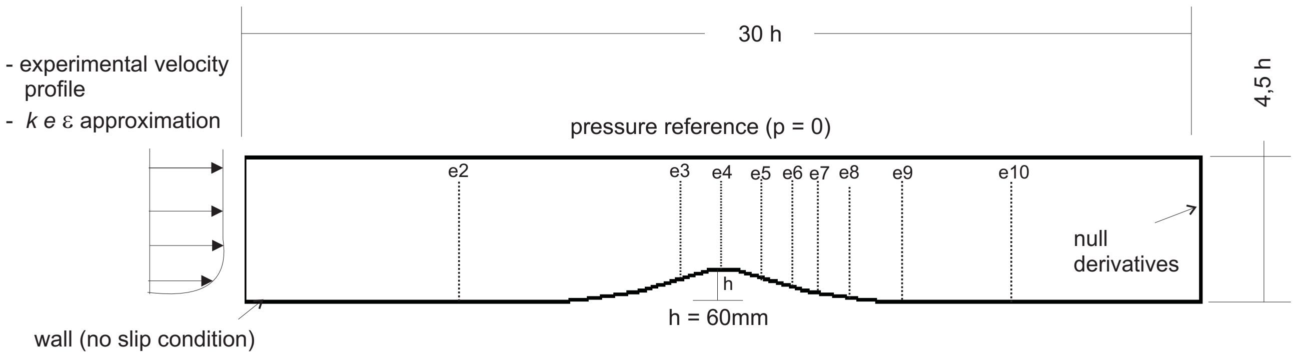


Figure 3. General outline of boundary conditions and geometrical characteristic.

the results obtained using smooth laws in Fig.(4), especially for law of Mellor (1966). In this location, there's no influence of the hill's shape and the mean longitudinal pressure gradient stay near zero.

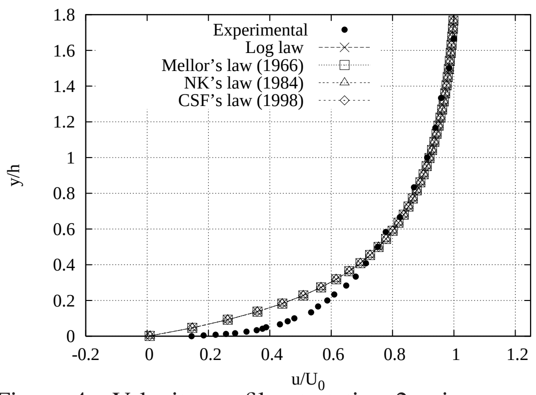


Figure 4. Velocity profile at station 2 using smooth laws.

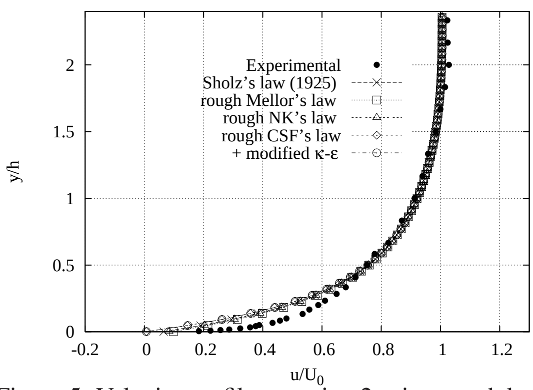


Figure 5. Velocity profile at station 2 using rough laws.

The station 4 represents the symmetric station, placed on hill's top. The strong fluid acceleration and logarithmic velocity profile were verified. Near wall region, the rough laws given the best results. This fact could be related to the friction velocity $u_F$ approximation.

The stations 5, 6 and 7 are inside the recirculation zone, downstream hill's top. The disturb due to boundary layer separation made the rough effects less perceptible. This way, the performance of the rough and smooth formulations was similar. For smooth laws, the law of Mellor (1966) was prominent, once consider the adverse pressure gradient effect. For rough laws, the prominent one is the law of Cruz and Silva Freire (1998) that runs associated to the modified form of $\kappa$-$\varepsilon$, proposed by Iaccarino and Gianluca (2001). This combination tends to Stratford's equation (1959) for separated flows.

Near the reattachment point, Fig. (15), the law of Sholz (1925) fails in predicting the velocity profile. However, the others rough laws showed agreement with the experimental data.

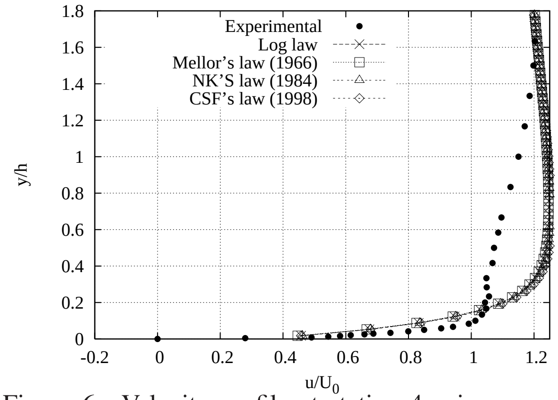


Figure 6. Velocity profile at station 4 using smooth laws.

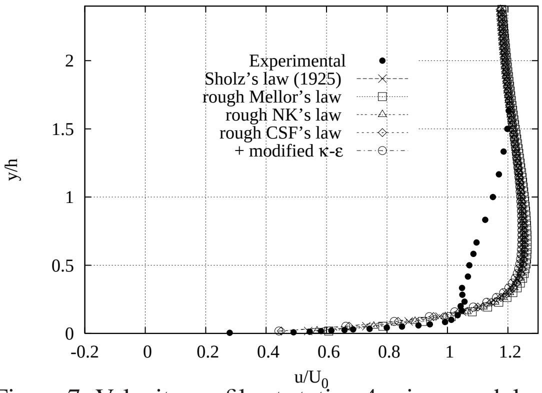


Figure 7. Velocity profile at station 4 using rough laws.

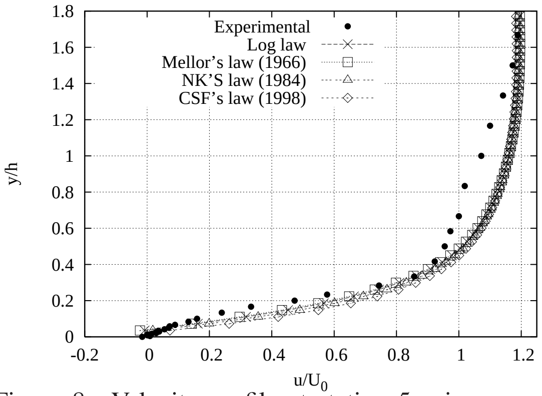


Figure 8. Velocity profile at station 5 using smooth laws.

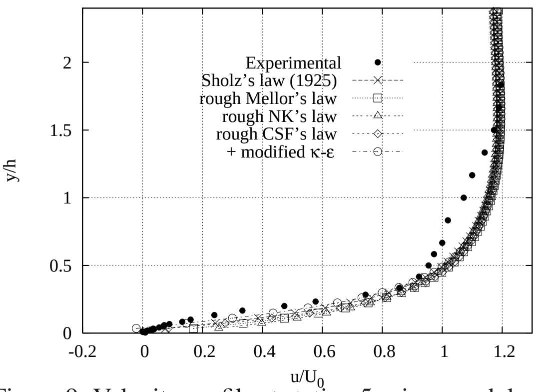


Figure 9. Velocity profile at station 5 using rough laws.

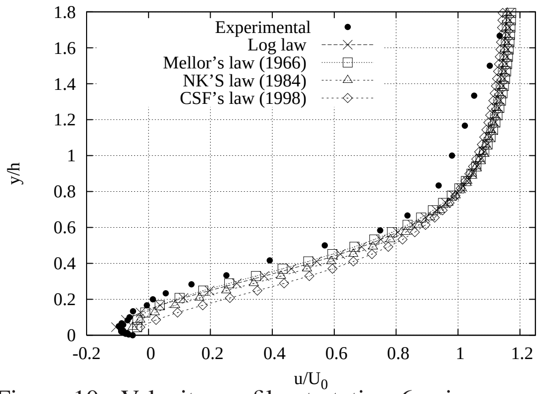


Figure 10. Velocity profile at station 6 using smooth laws.

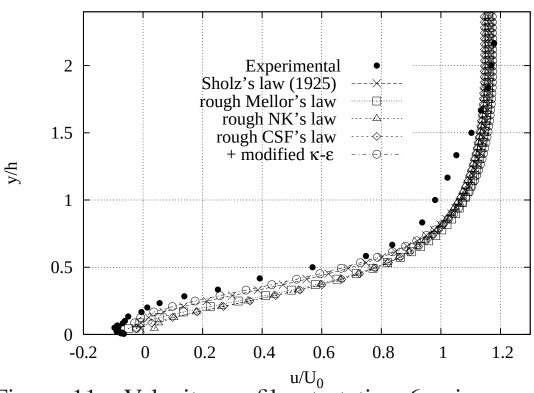


Figure 11. Velocity profile at station 6 using rough laws.

The longitudinal coefficient pressure gradient $C_p$, Fig. (16), Fig. (17) and Eq. (28), shows the strong gradient downstream hill's top. The flow pressure loss estimated, between inlet and exit numerical domain, is the same for each laws of the wall.

$$C_p = \frac{p - p_0}{\rho U_0^2} \tag{28}$$

$C_p$ is the longitudinal pressure gradient and $p_0$ is a reference pressure.

The friction velocity $u_F$ were showed at Fig.(18) and Fig.(19). The major values were found at hill's top, where the flow is more accelerated. In the upstream region, the rough laws' results were more efficient than smooth laws, except the law of Cruz and Silva Freire (1998), that showed agreement with the experimental data in this region. This fact confirmed the physical coherence of the rough scales adopted in the rough wall laws formulations.

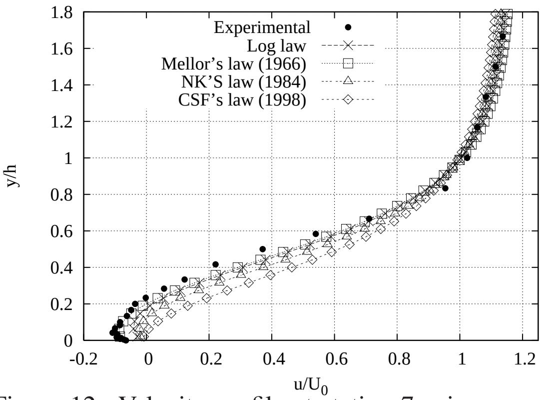


Figure 12. Velocity profile at station 7 using smooth laws.

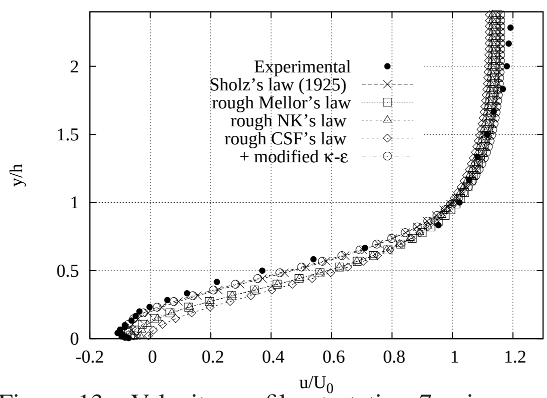


Figure 13. Velocity profile at station 7 using rough laws.

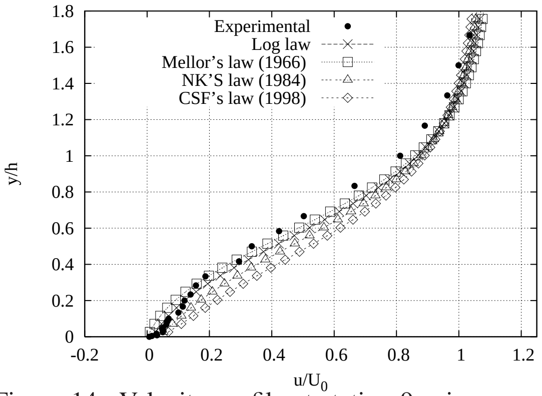


Figure 14. Velocity profile at station 9 using smooth laws.

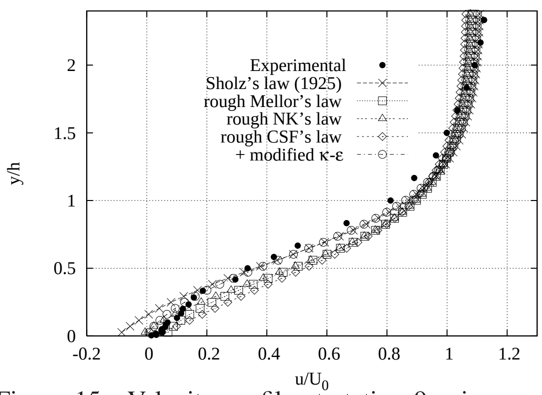


Figure 15. Velocity profile at station 9 using rough laws.

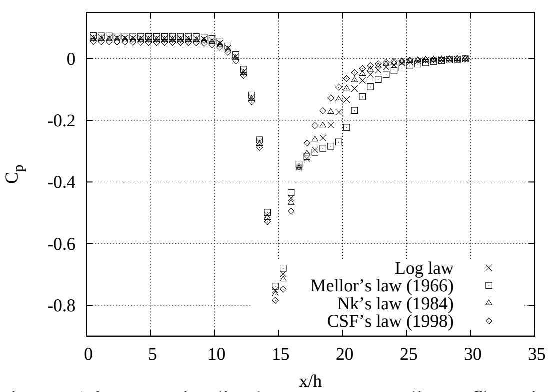


Figure 16. Longitudinal pressure gradient $C_p$ using smooth laws.

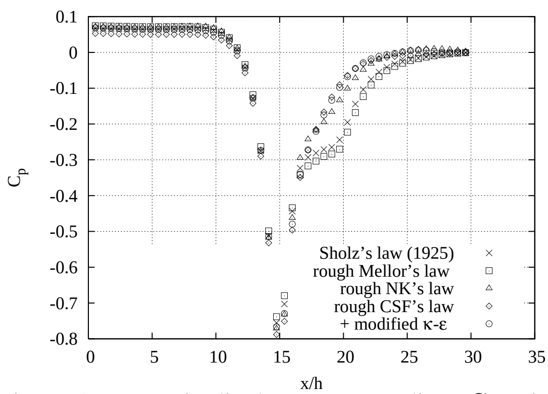


Figure 17. Longitudinal pressure gradient $C_p$ using rough laws.

## 5. CONCLUSIONS

The numerical results obtained with rough laws indicate a good agreement with the experimental results, especially in upstream and hill's top points. However, the downstream region were better simulated by using the modified form of $\kappa$-$\varepsilon$ associated to rough law of Cruz and Silva Freire (1998), due to the asymptotic condition of high pressure gradient and separated boundary layer.

The viscous sublayer destruction effect, observed in many experimental studies like Monteiro (2007) and Loureiro (2008), was successfully implemented in the laws of wall relations. The smooth laws of the wall had the performance improved when the error in origin concept $h_0$ was employed, replacing the numerical origin in order to consider the dynamic effects imposed to the flow by the roughness. Unfortunately, determinate the parameters $y_s$ and $h_0$ is not an easy task, because they depend on the roughness' geometrical characteristics and on the undisturbed flow settings.

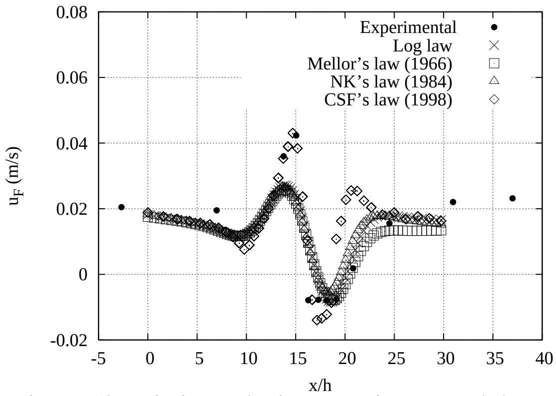


Figure 18. Friction velocity $u_F$ using smooth laws.

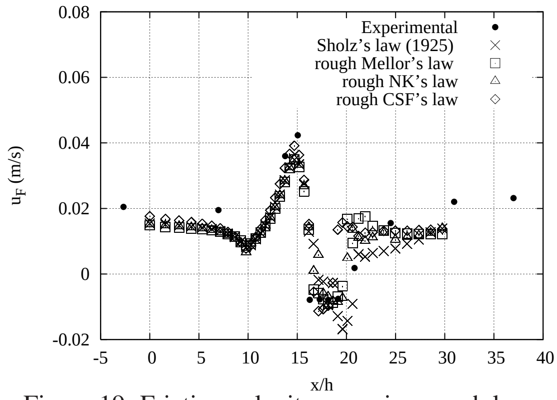


Figure 19. Friction velocity $u_F$ using rough laws.

This way, each kind of roughness has a particular pre-processing treatment. The shear stress, even being so difficult to experimentally measure or numerically estimate, was calculated using the minimization residual technique proposed by Fontoura Rodrigues (1991).

Finally, these results suggests that the $\kappa$-$\varepsilon$ limitations don't prohibit its use in flows with gradient pressures and separated boundary layers, associated or not to rough surfaces. However, in many cases a specific formulation is necessary for the near wall region.

## 6. REFERENCES

Buffat, M., 1981, "Formulation Moindres Carrt'es Adaptt'ees au Traitement des Effets Convectifs dans les Équations de Navier-Stokes", PhD thesis, Université Claude Bernard, France.

Cruz, D. O. A., Freire, A. P. S., 1998, "On single limits and the asymptotic behaviour of separating turbulent boundary layers", Inter. J. Heat and Mass Transfer, vol. 41, pp. 2097-2111.

Fontoura Rodrigues, J. L. A., 1990, "Méthode de Minimisation Adaptée à la Technique des Éléments Finis pour la Simulation des Et'coulements Turbulents avec Conditions aux Limites non Lint'eares de Proche Paroi", PhD thesis, Ecole Centrale de Lyon, France.

Hanjalic, K., Launder, B. E., 1972, "A Reynolds-stress model of turbulence and its applications to thin shear flows", Journal of Fluid Mechanics, vol. 52, n. 4, pp. 609-638.

Iaccarino, G., Poroseva, S., 2001, "Simulating separated flows using the $\kappa$-$\varepsilon$- model", Center for Turbulence Research, Annual Research Briefs 2001, pp. 375-383.

Ikeda T., Durbin, P. A., 2007, "Direct simulations of a rough-wall channel flow", Journal of Fluid Mechanics, vol. 571, pp. 235-263.

Jones, W. P., Launder, B. E., 1972, "The prediction of laminarisation with a two- equation model of turbulence", Journal of Heat and Mass Transfer, vol. 15, pp. 301-314.

Loureiro, J.B.R., Monteiro, A.S., Rodrigues, D.A., Alho, A.T.P., Pinho, F.T., Silva Freire, A.P., 2007a, "Law of the wall formulations for separating flow over rough surfaces", Proc. 19th Int. Congress of Mech. Eng. (COBEM 2007), Brasília-Brazil.

Loureiro, J.B.R., Soares, D.V., Fontoura Rodrigues, J.L.A., Pinho, F.T., Silva Freire, A.P., 2007b, "Water tank and numerical model studies of flow over step smooth two-dimensional hills", Boundary-Layer Meteorol, 122, 343-365.

Loureiro, Juliana Braga Rodrigues, 2008, "Escoamento turbulento sobre colinas abruptas lisas e rugosas com extensas regiões de separação" , COPPER UFRJ- Tese de Doutorado, Rio de Janeiro-Brazil.

Mellor, G. L., 1966, "The effects of pressure gradients on turbulent flow near a smooth wall", Journal of Fluid Mechanics, vol. 3, n. 2, pp. 140-150.

Monteiro, A.S., Loureiro, J. B. R., Pinho, F. T., Silva Freire, A. P., (2006) "Flow over a steep rough hill". Proc. 11th Braz. Cong. Of Thermal Sci. and Eng., ENCIT 2006, Curitiba - Brazil

Monteiro, A.S., 2007, "Estudo experimental de escoamentos turbulentos sobre colinas bidimensionais rugosas", Dissertação de Mestrado, pp 127, Programa de Engenharia Mecânica, COPPE/UFRJ - Brazil.

Nakayama, A., Koyama, H., 1984, "A wall law for turbulent boundary layers in adverse pressure gradients", AIAA Journal, vol.24.

Nikuradse, J., (1933) "Stromungsgesetzein Rauhen Rohren". V. D. I. Forshungsheft 361

Perry, A. E., Joubert P.N., 1963, "Rough-wall boundary layers in adverse pressure gradients", Journal of Fluid Mechanics, vol. 17, pp. 193-211.

Stratford, B. S., 1959, "The prediction of separation of the turbulent boundary layer", Journal of Fluid Mechanics, vol. 5, pp.1-16.

Soares, D.V., Fontoura Rodrigues, J.L.A., 2005, "The numerical simulation of a turbulent flow over a two dimensional hill", 2005,Proceedings of the XXVI Iberian Latin-American Congress on Computational Methods in Engineering - CILAMCE 2005, Guarapari -Espírito Santo - Brazil.

Townsend, A. A., 1960, "Equilibrium layers and wall turbulence", Cambridge University Press.